Decomposing the risk of algorithmic portfolios

Nabil Bouamara[a,b,*], Kris Boudt[b,c,d], Jürgen Vandenbroucke[e,f,g]

[a]*Department of Accounting, Finance and Insurance, KU Leuven, Naamsestraat 69, 3000 Leuven, Belgium*
[b]*Solvay Business School, Vrije Universiteit Brussel, Pleinlaan 2, 1050 Brussels, Belgium*
[c]*Department of Economics, Ghent University, Sint-Pietersplein 6, Ghent, Belgium*
[d]*School of Business and Economics, Vrije Universiteit Amsterdam, De Boelelaan 1105, 1081 HV Amsterdam, The Netherlands*
[e]*KBC Asset Management, Havenlaan 2, 1080 Brussels, Belgium*
[f]*Department of Business and Economics, University of Antwerp, Prinsstraat 13, 2000 Antwerpen, Belgium*
[g]*EDHEC–Risk Institute, 393-400 Promenade des Anglais, BP 3116, 06202 Nice Cedex 3, France*

January 25, 2022

Abstract

Sophisticated algorithmic techniques are complementing human judgement across the fund industry. Whatever the type of rebalancing that occurs in the course of a longer horizon, it probably violates the buy-and-hold assumption. In this article, we develop the methodology to predict, dissect and interpret the h-day financial risk in algorithmic portfolios. Our risk budgeting approach is based on a flexible risk factor model that accommodates the dynamics in portfolio composition directly within the risk factors. Once these factors are defined, we cast portfolio risk measures, such as value-at-risk, into an additive mean-variance-skewness-kurtosis format. The simulation study confirms the gains in accuracy compared to the widespread square-root-of-time rule. Our main empirical findings rely on the two-decade performance of a portfolio insurance investment strategy. Rather than looking at total portfolio risk, we conclude that it is more informative to look inside the portfolio.

Keywords: Co-moments; Decomposition; Fund management; Risk management; Risk factors; Square-root-of-time
JEL classification: C100, C150, G110

1. Introduction

One of the fastest growing innovations in the asset management industry uses algorithms and machine learning techniques to find profitable patterns in market data.[1] A tension arises linked to the feature that the portfolio composition tends to change frequently across the risk evaluation horizon, naturally suggesting the

*Corresponding author. Tel.: +32-2-629 2428. *E-mail addresses:* nabil.bouamara@kuleuven.be (Nabil Bouamara), kris.boudt@ugent.be (Kris Boudt), jurgen.jv.vandenbroucke@kbc.be (Jürgen Vandenbroucke). *Acknowledgements:* We are grateful to KBC Asset Management's R2 team for generously sharing their expertise on portfolio insurance strategies. We have received helpful comments and suggestions from Andres Algaba, David Ardia, Samuel Borms, Leopoldo Catania, Serge Darolles, Hans Degryse, Jean-Yves Gnabo, Geert Huyghe, Olivier Scaillet, Piet Sercu, Thiago de Oliviera Souza, James Thewissen, Tim Vanvaerenbergh, Jens Verbrugge as well as the participants at the Mathematical and Statistical Methods for Actuarial Sciences and Finance Conference (Madrid, 2018), the European Actuarial Journal Conference (Leuven, 2018), the Conference in International Macroeconomics and Financial Econometrics (Nanterre, 2019), the KU Leuven seminars, the Quantitative Finance and Financial Econometrics Conference (Marseille, 2019), the Society of Financial Econometrics Summer School (Brussels, 2018; Evanston, 2019) and the International Conference of the French Finance Association (Online, 2021). This work was supported by the Research Foundation – Flanders [PhD fellowship 11F8419N].

use of risk signalling tools on each single trade. On the other hand, it is more realistic to rely on aggregated information on lower-frequency intervals. This turns out to be even more problematic because the classical approaches to understand risk over a longer-horizon are predicated on the buy-and-hold assumption, or equivalently, that the timing of risk evaluation and portfolio allocation coincide.

In this article, we focus on the insights afforded by Litterman (1996)'s "hot spots" – a traditional tool to reveal how much of the total portfolio risk can be attributed to underlying building blocks, such as sectors, asset classes, geographical regions, etc. Our main methodological contribution is that we account for the mismatch between the risk evaluation horizon and the frequency of investment decisions. We do so by accommodating the random nature of the intra-window composition directly within the risk factors, allowing for a direct description of *non-buy-and-hold* portfolios. We impose some structure on the time-varying position vector by defining it within a flexible class of data-driven investment strategies, which includes any investment that is mechanically driven by past price movements. Furthermore, to dissect and interpret financial risk, we consider mean-variance-skewness-kurtosis (MVSK) portfolio risk measures, i.e. closed-form expressions of the exposure vector and the portfolio co-moments (i.e., co-variance, co-skewness and co-kurtosis). An intuitive, two-dimensional companion table is meant to illustrate how, vertically, the risks of the factors add up to create the risk of the portfolio and, horizontally, portfolio and factor risk can be decomposed into Gaussian and non-Gaussian attributes.

We contribute to the literature in two ways. First, we introduce risk factors for active investment strategies. A similar motivation for the use of strategy-based returns can be found in Fung and Hsieh (2001), who propose a single option-like factor that captures the characteristics of the entire family of trend-following hedge funds. Our approach is distinctly different in that we incorporate the specific aspects of the investment strategy directly into the assets. In doing so, we offer a multi-period portfolio analysis tool for individual investors that relates each observable portfolio component (e.g. Dow 30 constituents) directly to a manageable set of risk factors. Second, we contribute to the interpretability of risk measure. Much of the recent literature has focused the sensitivity of tail risk to portfolio moments Stoyanov et al. (2013a,b), dynamic portfolio risk (Francq and Zakoïan, 2018), dynamic asset allocation models (Baştürk et al., 2019) and portfolio optimization with non-Gaussian objectives (see e.g. Boudt et al., 2020a,b). The idea that active rebalancing does not merely result in the shift of the marginal risk impacts but completely transforms the structural relationship between individual companies, requires us to look inside the portfolio. In particular, we offer a complementary picture of risk in a portfolio, treating portfolio risk as the result of different combinations of factors and their interactions.

In the empirical application, we investigate the expected shortfall of active positions in the 30 Dow Jones Industrial Average constituents. Specifically, we examine a Constant-Proportion Portfolio Insurance (CPPI) investment algorithm, similar to the CPPI products sold to European retail investors.[2] Previous research by Ardia et al. (2016) has concluded that, due to the non-linear and multi-horizon nature of this investment, its path dependence and the asymmetric impact of volatility, it is not immediately obvious how the risk characteristics of the underlying components affect the performance of the investment. In response, we find that our portfolio analysis tool overcomes these problems and allows for a better judgement as to how the shape of the left tail is affected through each component.

The remainder of this article is structured as follows. Section 2 sets out a general framework for the decomposition of MVSK portfolio risk, which nests any data-driven portfolio strategy and investment horizon. Section 3 is concerned with practical guidelines and sketches a simple step-by-step procedure for risk budgeting a portfolio. The simulated results in Section 4 confirm our intuition that the naive square-root-of-time rule is inappropriate for dynamic portfolios. Section 5 discusses the empirical results of MVSK risk measures to gauge the risk of active Dow 30 portfolios over the period 1987 to 2009. We conclude in Section 6.

2. Methodology for long-horizon risk decomposition

Figure 1 sets out the main idea. The investor has the responsibility to gauge ex-ante risk over the multi-period horizon, while being aware that the investment rule may actively rebalance the portfolio at a set of potential rebalancing points, indicated by $t = 0, 1, 2, ..., h$.

Figure 1: Risk evaluation intervals *vs.* portfolio rebalancing intervals

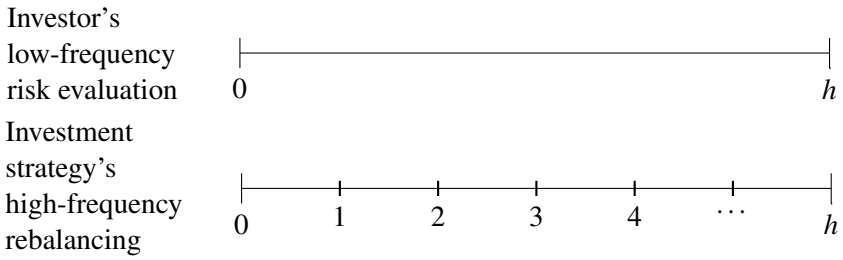

Note: We visualize the low-frequency risk evaluation interval vs. higher-frequency portfolio decision interval. The investor gauges risk over the h-period horizon (top panel), while being aware that the investment rule may actively rebalance the portfolio at a set of potential rebalancing points, indicated by $t = 0, 1, 2, ..., h$ (bottom panel).

This section introduces the methodology for long-horizon risk decomposition in all its generality. We begin in Section 2.1 by making the explicit distinction between longer-horizon risk evaluation and shorter-horizon portfolio rebalancing intervals. We also propose a model that will be central to disentangle longer-horizon portfolio risk across factors. In Section 2.2 we introduce our MVSK risk measure. In Section 2.3, we map the risk measure into factors and MVSK contributions. Finally, in Section 2.4, we include an illustration of the MVSK decomposition using a stylistic example.

2.1. Notation

Let $r_{i,t}$ be the intra-window log-returns of the i–th asset at time t, respectively for $i = 1, ..., p$ and $t = 1, ..., h$. We normalize the horizon h to be a risk evaluation interval. The portfolio log-returns $y_t(w_{t-1})$ are equal to

$$y_t(\boldsymbol{w}_{t-1}) \;=\; \log\left(\sum_{i=1}^{p} w_{i,t-1} e^{r_{i,t}}\right), \quad \text{for } 1 \leq t \leq h \text{ and } i = 1, 2, ..., p. \tag{1}$$

The time-subscript in the component weights $\boldsymbol{w}_{t-1}$ highlights the portfolio is rebalanced using past information.

We impose that the investment portfolio log-returns $y_t(\boldsymbol{w}_{t-1})$ adhere to a data-driven system. More formally, the intra-window weights are defined by

$$\boldsymbol{w}_t \quad = u(\boldsymbol{r}_{1:t-1}, \boldsymbol{w}_{t-1}; \boldsymbol{\omega}), \tag{2}$$

in which the $u(\cdot)$ function is an updating equation. The static parameter vector $\boldsymbol{\omega}$ defines the characteristics of the investment strategy and thus defines the type of updating used for $\boldsymbol{w}_t$. The recursive nature of the formulation implies that $u(\boldsymbol{r}_{1:t-1}, \boldsymbol{w}_{t-1}; \boldsymbol{\omega})$ is path-dependent – it is a function of the multivariate history of p-dimensional of asset returns $\boldsymbol{r}_{1:t-1} \equiv \{\boldsymbol{r}\}_1^{t-1}$, weights $\boldsymbol{w}_{t-1}$ and possibly other exogenous variables.

Notable examples that fit into this data-driven framework include momentum or relative-strength strategies that buy past winners and sell past losers, contrarian strategies that exploit reversal trades, fundamental value portfolios, the family of risk-based portfolios (inverse volatility, minimum variance, maximum diversification, equally weighted, etc.), technical trading rules, so-called "smart beta" strategies, portfolio insurance techniques, and the more recent techniques leveraging articifical intelligence criteria (see e.g. De Prado, 2018, for a broad treatment).

The return across the risk evaluation window, or the h-period portfolio log-return, is the sum of one-step log-returns

$$y^h \quad := \quad \sum_{t=1}^{h} y_t(\boldsymbol{w}_{t-1}). \tag{3}$$

Now we turn to the linear connection between the longer-horizon portfolio return y^h and the underlying building blocks, which is central in the subsequent equations. A convenient way to describe the multi-period portfolio return of an active p-asset portfolio is a factor model

$$y^h = \alpha + \boldsymbol{f}'\boldsymbol{a}, \tag{4}$$

in which α is the intercept, $\boldsymbol{a} = (a_1, ..., a_q)'$ is the exposure vector consisting of factor loadings and $\boldsymbol{f} = (f_1, ..., f_q)'$ is the q-dimensional factor variable. The benefit of this structure is that it is now possible to decompose portfolio risk for horizons longer than the frequency at which portfolios are rebalanced. As we will show later in this paper, additional granularity is possible by casting portfolio returns in a mean-variance-skewness-kurtosis format. Therefore, $\boldsymbol{f}$ is assumed to have finite fourth-order moments.

Several approaches exist to select the risk factors $\boldsymbol{f}$. In financial applications, the assumption of macro-economic, fundamental and statistical models in multi-factor models is common (see, for example, Connor, 1995). Without loss of generality, we use synthetic risk factors that mimic and accommodate the portfolio fluctuations of the corresponding investment strategy across a longer horizon. We refer to Section 3.1 for further elaboration.

2.2. Portfolio risk

To dissect and interpret financial risk, we require a multivariate risk function ρ that can be expressed as a closed form of the exposure vector $\boldsymbol{a}$ and the co-moments of the risk factors $\boldsymbol{f}$ (i.e. the mean vector $\boldsymbol{\mu}$, the

co-variance matrix $\mathbf{\Sigma}$, the co-skewness matrix $\mathbf{\Phi}$ and the excess[3] co-kurtosis matrix $\mathbf{\Psi}$)

$$\rho(\boldsymbol{a};\boldsymbol{\mu},\mathbf{\Sigma},\mathbf{\Phi},\mathbf{\Psi}), \tag{5}$$

in which $\rho(\boldsymbol{a};\boldsymbol{\mu},\mathbf{\Sigma},\mathbf{\Phi},\mathbf{\Psi})$ is a one-homogeneous function of $\boldsymbol{a}$.[4] We refer to Appendix A for the necessary formulas to calculate the co-moments.

Examples of risk functions nested in Eq. (5) include the portfolio standard deviation, portfolio value-at-risk and portfolio expected shortfall. Non-normal features in financial returns can be accounted for via Cornish-Fisher value-at-risk (Zangari, 1996) and Edgeworth expected shortfall (Boudt et al., 2008). The former relies on Cornish-Fisher expansions around the standard Gaussian quantile funtion and the latter on Edgeworth expansions around the standard Gaussian distribution function. The use of asymptotic expansions in calculating left-tail risk has been well-studied in the literature. For example, Zoia et al. (2018) make use of Gram-Charlier expansions to calculate value-at-risk and expected shortfall. We refer to Appendix B for a comprehensive definition of these risk measures.

2.3. Two-dimensional mean-variance-skewness-kurtosis risk attribution

We focus on the part of the overall risk that should be the object of concern in risk management or asset allocation, along the lines of Litterman (1996, p. 92), i.e. "the practice of risk managers needs to reflect that what matters is the marginal impact on the risk of the portfolio, not the risk of the individual securities."

Since the portfolio return is defined as a linear function of factors (see Eq. 4), it follows that the portfolio risk measure is a *one-homogeneous* function of the portfolio exposure vector $\boldsymbol{a}$. Risk factor decomposition is then straightforward via Euler's Homogeneous Function Theorem (see Gourieroux et al., 2000; Scaillet, 2004, for examples).

The Euler Theorem for dynamic portfolios is formulated in the following equation. For portfolio returns y^h described by exposure vector $\boldsymbol{a}$ and the q-dimensional risk factor set $\boldsymbol{f}$, we have a top-down attribution of total portfolio risk to the part that can be attributed to risk factors

$$\rho(\boldsymbol{a};\cdots) = \sum_{j=1}^{q} a_j \, \partial_j \rho(\boldsymbol{a};\cdots), \tag{6}$$

in which $\partial_j \rho(\boldsymbol{a};\cdots) = \partial \rho(\boldsymbol{a};\cdots)/\partial a_j$ is the partial derivative of the portfolio risk with respect to the exposure to the risk factor j. The contribution of factor j over the same risk evaluation window is equal to $\rho_j(\boldsymbol{a};\cdots) = a_j \partial_j \rho(\boldsymbol{a};\cdots)$. Similarly, the percentage contribution is defined as $\%\rho_j(\boldsymbol{a};\cdots) = \rho_j(\boldsymbol{a};\cdots)/\rho(\boldsymbol{a};\cdots)$. We use the dots shorthand to save space.

Aside from a decomposition into factors, the ability to decompose the portfolio risk into its Gaussian and non-Gaussian characteristics is also useful for explaining the sources of risk. In this vein Andreas Steiner proposes in a white paper to disentangle portfolio modified value-at-risk into additive mean, standard

deviation, skewness and kurtosis contributions[5]

$$\begin{aligned}
\text{mVaR}(\boldsymbol{a};\cdots) &:= \text{mVaR}^{\mu}(\boldsymbol{a};\cdots)+\text{mVaR}^{\sigma}(\boldsymbol{a};\cdots)+\text{mVaR}^{s}(\boldsymbol{a};\cdots)+\text{mVaR}^{k}(\boldsymbol{a};\cdots), && \text{(7a)}\\
\text{with,} && && \text{(7b)}\\
\text{mVaR}^{\mu}(\boldsymbol{a};\cdots) &:= -\mu, && \text{(7c)}\\
\text{mVaR}^{\sigma}(\boldsymbol{a};\cdots) &:= -\sigma z_{\alpha}, && \text{(7d)}\\
\text{mVaR}^{s}(\boldsymbol{a};\cdots) &:= -\sigma\left[1/6(z_{\alpha}^{2}-1)s-1/36(2z_{\alpha}^{3}-5z_{\alpha})s^{2}\right], && \text{(7e)}\\
\text{mVaR}^{k}(\boldsymbol{a};\cdots) &:= -\sigma[1/24(z_{\alpha}^{3}-3z_{\alpha})k], && \text{(7f)}
\end{aligned}$$

in which, z_{α} is the standard Gaussian quantile, μ is the portfolio mean, σ is the portfolio volatility, s is the portfolio skewness and k is the portfolio kurtosis. Each subequation corresponds to the mean, volatility, skewness and kurtosis contributions to total modified value-at-risk, respectively.

We find that similar results hold for many other risk functions of the form defined in Eq. (5). More precisely, we propose a generalized decomposition in which portfolio risk is mapped into a mean-variance-skewness-kurtosis framework by calculating the marginal effect of each moment contribution

$$\begin{aligned}
\rho := &\quad \rho^{\mu}+\rho^{\sigma}+\rho^{s}+\rho^{k}, \quad \text{with,} && && \text{(8a)}\\
\rho^{\mu} := &\quad \rho\left(\boldsymbol{a};\boldsymbol{\mu},\mathbf{0}_{q\times q},\mathbf{0}_{q\times q^{2}},\mathbf{0}_{q\times q^{3}}\right) && -\rho\left(\boldsymbol{a};\mathbf{0}_{q\times 1},\mathbf{0}_{q\times q},\mathbf{0}_{q\times q^{2}},\mathbf{0}_{q\times q^{3}}\right), && \text{(8b)}\\
\rho^{\sigma} := &\quad \rho\left(\boldsymbol{a};\boldsymbol{\mu},\boldsymbol{\Sigma},\mathbf{0}_{q\times q^{2}},\mathbf{0}_{q\times q^{3}}\right) && -\rho\left(\boldsymbol{a};\boldsymbol{\mu},\mathbf{0}_{q\times q},\mathbf{0}_{q\times q^{2}},\mathbf{0}_{q\times q^{3}}\right), && \text{(8c)}\\
\rho^{s} := &\quad \rho\left(\boldsymbol{a};\boldsymbol{\mu},\boldsymbol{\Sigma},\boldsymbol{\Phi},\mathbf{0}_{q\times q^{3}}\right) && -\rho\left(\boldsymbol{a};\boldsymbol{\mu},\boldsymbol{\Sigma},\mathbf{0}_{q\times q^{2}},\mathbf{0}_{q\times q^{3}}\right), && \text{(8d)}\\
\rho^{k} := &\quad \rho\left(\boldsymbol{a};\boldsymbol{\mu},\boldsymbol{\Sigma},\boldsymbol{\Phi},\boldsymbol{\Psi}\right) && -\rho\left(\boldsymbol{a};\boldsymbol{\mu},\boldsymbol{\Sigma},\boldsymbol{\Phi},\mathbf{0}_{q\times q^{3}}\right), && \text{(8e)}
\end{aligned}$$

in which $\mathbf{0}_{\cdot\times\cdot}$ is a zero matrix, the superscript of ρ^{m}, with moment $m\in\{\mu,\sigma,s,k\}$. Each subequation corresponds to the mean, volatility, skewness and kurtosis contributions to total risk, respectively. For example, the generalization naturally extends to the portfolio modified expected shortfall originally proposed by Boudt et al. (2008), which involves complex products of density functions.

Finally, we wish to see how each of the factors affects the portfolio-level moment budgets in Eqs. (8a – 8e). We simply apply Euler's Theorem on each of the one-homogeneous subequations.

Table 1 depicts the concept of two-dimensional risk attribution to factors and moments. The elements

$$\rho_{j}^{m} := a_{j}\,\partial_{j}\rho^{m}, \quad \text{for } j=1,...,q \text{ and } m\in\{\mu,\sigma,s,k\}, \tag{9}$$

represent the contribution of factor j to the conditional moment contribution $c_{m}\rho$ (viz., Eqs. (8b) through (8e)). The partial derivative $\partial_{j}c_{m}\rho(\boldsymbol{a},\boldsymbol{\mu},\boldsymbol{\Sigma},\boldsymbol{\Phi},\boldsymbol{\Psi})$ is the moment contribution of the partial derivative with respect to the exposure to a particular risk factor. Note that $\sum_{m}\rho_{j}^{m}=\rho_{j};\sum_{j}\rho_{j}^{m}=\rho_{m};\sum_{j}\rho_{j}=\sum_{m}\rho^{m}=\rho;\sum_{j}\sum_{m}\rho_{j}^{m}=\rho$.

It can be seen that the companion table reflects three levels of diagnostic information: portfolio, factor and moment. In the bottom-right, we report the total risk of a portfolio. Vertically, total risk is decomposed

Table 1: Mean-variance-skewness-kurtosis risk budgeting table

Factor \ Moment	Contributions: Mean	St.Dev.	Skewness	Kurtosis	Total
Factor_1	ρ_1^{μ}	ρ_1^{σ}	ρ_1^{s}	ρ_1^{k}	ρ_1
Factor_2	ρ_2^{μ}	ρ_1^{σ}	ρ_2^{s}	ρ_2^{k}	ρ_2
Factor_3	ρ_3^{μ}	ρ_3^{σ}	ρ_3^{s}	ρ_3^{k}	ρ_3
$\vdots$	$\vdots$	$\vdots$	$\vdots$	$\vdots$	$\vdots$
Factor_j	ρ_j^{μ}	ρ_j^{σ}	ρ_j^{s}	ρ_j^{k}	ρ_j
$\vdots$	$\vdots$	$\vdots$	$\vdots$	$\vdots$	$\vdots$
Factor_q	ρ_q^{μ}	ρ_q^{σ}	ρ_q^{s}	ρ_q^{k}	ρ_q
Total	ρ^{μ}	ρ^{σ}	ρ^{s}	ρ^{k}	ρ

Note: We propose a tabular form for the decomposition of mean-variance-skewness-kurtosis risk $\rho := \rho^{\mu} + \rho^{\sigma} + \rho^{s} + \rho^{k}$, itself made up of factor contributions defined ρ_j^m, with $j = 1, ..., q$ and $m \in \{\mu, \sigma, s, k\}$. We make use of a simple rectangle tabular structure to illustrate how, vertically, the risks of the components add up to create the risk of the portfolio and, horizontally, portfolio and component risk can be decomposed into normal and non-normal attributes.

into the risk contribution of each risk factor position. Horizontally, total risk and each factor contribution are disentangled into the effects of traditional moments. By construction, these contributions add up to total portfolio risk.

2.4. A glance at the mean-variance-skewness-kurtosis risk measure

The two-panel illustration in Figure 2 is meant to clarify the ideas in the previous subsection.

In Panel (a), we show four left tails of Edgeworth *pdf*s that illustrate differences in portfolio return characteristics (i.e. mean, volatility, skewness and kurtosis). We make sure that these portfolios have an identical 5% portfolio modified expected shortfall (mES) equal to 1.459 by rescaling the volatility (see the location-scale representation in Eq. (24)).

We call these stylized examples "seemingly iso-risk portfolios" to emphasize that, while these portfolios have exactly the same *aggregate portfolio risk*, their inherent risk profiles are very different. This can also be observed visually through the markedly different formations of the left tail. For example, in investment Strategy B, large negative observations are more likely to appear than large positive realizations ($s = -0.500$). In addition, the return distribution has a tail that may not vanish as quickly as those expected from a normal distribution ($k = 1.000$).

It is well-known that investors are averse to negative skewness and positive kurtosis (Scott and Horvath, 1980). Unfortunately, these standard analytics available in the risk manager's information set do not provide an adequate basis for understanding and managing the portfolio.

Panel (b) emphasizes the role by the respective components as a way to reveal additional information about the inherent interactions within the same portfolios. As noted before, we provide a complementary picture of the risk, treating portfolio risk not simply as a univariate observation, but rather as the result of

Figure 2: Mean-variance-skewness-kurtosis factor attribution for seemingly iso-risk portfolios

(a) Iso-risk in different portfolio return density functions

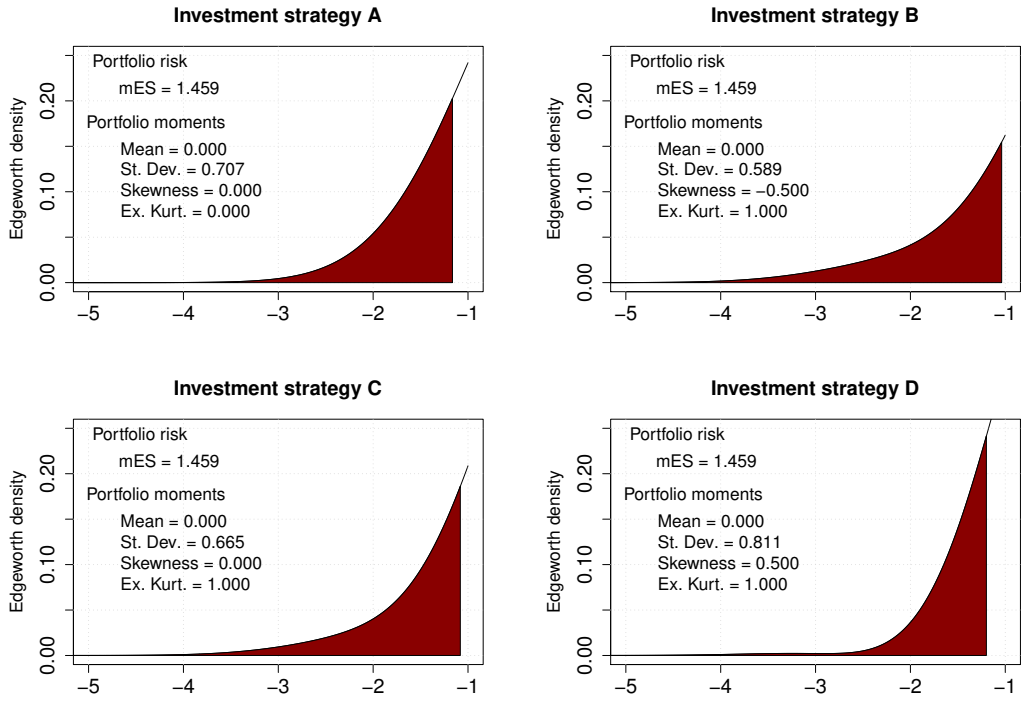

(b) Mean-variance-skewness-kurtosis decomposition of portfolio risk (in %)

Factor \ Moment	Modified expected shortfall contributions (%)				
	Mean	St.Dev.	Skewness	Kurtosis	Total
Investment strategy A					
Factor_1	0.000	0.729	0.000	0.000	0.729
Factor_2	0.000	0.729	0.000	0.000	0.729
Total	0.000	1.459	0.000	0.000	**1.459**
Investment strategy B					
Factor_1	0.000	0.607	0.109	0.231	0.947
Factor_2	0.000	0.607	−0.001	−0.094	0.512
Total	0.000	1.214	0.107	0.138	**1.459**
Investment strategy C					
Factor_1	0.000	0.686	0.000	0.081	0.767
Factor_2	0.000	0.686	0.000	0.005	0.691
Total	0.000	1.372	0.000	0.087	**1.459**
Investment strategy D					
Factor_1	0.000	0.836	−0.446	−0.123	0.268
Factor_2	0.000	0.836	0.210	0.144	1.191
Total	0.000	1.673	−0.235	0.021	**1.459**

Note: In the top panel, we analyze risk for portfolios with the same total portfolio risk. We visualize modified expected shortfall (red) for the Edgeworth density for different combinations of the traditional moments. The target expected shortfall is that of a normal distribution. In the bottom panel, we show the diagnostic MVSK table of the same iso-risk portfolios. We propose a tabular form for the decomposition of total risk (in bold) across factor contributions (vertically) and across moment contributions (horizontally). We assume independent risk factors.

different factor contributions. In fact, every expected shortfall can be endlessly expressed as the sum of four traditional portfolio moment contributions, themselves made up of additive factor contributions (see Eq. (9)). In addition, the multivariate interactions among the portfolio's factors are equally endless. After all, different entries in the co-variance, co-skewness or co-kurtosis matrices can lead to similar levels of total portfolio risk.

For simplicity of exposition, we consider a bivariate portfolio with independent factor components. For instance, the co-moments that were used to obtain Investment strategy D is equal to,

$$
\begin{aligned}
\boldsymbol{\mu} &= \begin{pmatrix} 0.000 \\ 0.000 \end{pmatrix}; \\
\boldsymbol{\Sigma} &= \begin{pmatrix} 1.000 & 0.000 \\ 0.000 & 1.000 \end{pmatrix}; \\
\boldsymbol{\Phi} &= \begin{pmatrix} 1.525 & 0.000 & 0.000 & 0.000 \\ 0.000 & 0.000 & 0.000 & -0.110 \end{pmatrix}; \\
\boldsymbol{\Psi}^{*} &= \begin{pmatrix} 4.000 & 0.000 & 0.000 & 1.500 & 0.000 & 1.500 & 1.500 & 0.000 \\ 0.000 & 1.500 & 1.500 & 0.000 & 1.500 & 0.000 & 0.000 & 3.000 \end{pmatrix}
\end{aligned}
$$

The parameters for the other investment strategies are available upon request.

In what follows we discuss some interesting results in these iso-risk portfolios. In the Gaussian investment strategy A, we make two trivial observations. First, as can be seen in the utmost right column, each asset contributes equally to the total portfolio risk ($\rho_1 = \rho_2 = 0.729$). Second, the portfolio risk profile can be described completely by mean and variance contributions ($\rho^s = \rho^k = 0.000$).

The other investment strategies are characterized by different combinations of skewness and excess kurtosis. For example, the univariate return distribution of Strategy D has a portfolio return distribution that is described by positive skewness ($s = 0.500$) and positive excess kurtosis ($k = 1.000$). Correspondingly, in the bottom panel, we observe that portfolio risk is affected by a negative skewness contribution ($\rho^s = -0.235$), lowering portfolio risk, and a positive kurtosis contribution ($\rho^k = 0.021$), increasing portfolio risk.

If we dig deeper, we see that the lion's share of total portfolio risk is driven by Factor$_2$ ($\rho_2 = 1.191$) with non-Gaussian attributes that increase portfolio risk ($\rho_2^s = 0.210$, $\rho_2^k = 0.144$). In comparison to Strategy B, the roles of Factor$_1$ and Factor$_2$ are reversed, albeit with different amounts ($\rho_1 = 0.947$, $\rho_2 = 0.512$). This shows that the risk attribution report, which is complementary to existing portfolio analysis tools, endows portfolio risk with richer information and potentially different economic interpretations.

3. Implementation

The implementation of the proposed risk budgeting methodology requires to estimate the exposure vector ($\boldsymbol{a}$), multivariate moments ($\boldsymbol{\mu}, \boldsymbol{\Sigma}, \boldsymbol{\Phi}, \boldsymbol{\Psi}$), and portfolio risk ($\rho$). We propose the Simulation-based Multi-period Portfolio Attribution (SiMPA) algorithm, which is a three-step procedure for risk budgeting a class of investment strategies that may trade within the risk prediction horizon.

3.1. Construction of the data matrices

In this subsection we elaborate on the practical considerations of associating the weight updating equation defined in Eq. (2) proportionally with the underlying components across a longer-horizon risk evaluation interval.

We assume to have a fully specified simulation model for the daily asset returns. An example of such a model is given in Appendix C. Denote the simulated daily data by $\tilde{\boldsymbol{r}}_t = (\tilde{\boldsymbol{r}}_{1,t}, ..., \tilde{\boldsymbol{r}}_{n,t})'$ with $\tilde{\boldsymbol{r}}_{i,t} \in \mathbb{R}^p$ a sample of p-dimensional observations of the asset log-return variable at time t.

The portfolio composition is path-dependent, meaning that it is conditional on the multivariate lagged series of assed returns and lagged asset weights (see Eq. (2)). For each time index t in the prediction horizon, we apply a data-driven investment rule (described by the updating equation) on asset return draws. After applying Eq. (1), this leads to rebalanced daily portfolio returns $\tilde{\boldsymbol{y}}_t = (\tilde{y}_{1,t}, ..., \tilde{y}_{n,t})'$ described by a set of intra-window active weights $\tilde{\boldsymbol{w}}_{t-1} = (\tilde{\boldsymbol{w}}_{1,t-1}, ..., \tilde{\boldsymbol{w}}_{n,t-1})'$, in which $\tilde{\boldsymbol{w}}_{i,t-1}$ is a sample of p-dimensional observations of component weights.

In order to construct style risk factors, we correct the simulated asset returns for the intra-window composition fluctuations via *pairwise multiplication* between component weights $\tilde{\boldsymbol{w}}_{t-1}$ and simple asset returns $(\exp(\tilde{\boldsymbol{r}}_t) - 1)$, leading to $\tilde{\boldsymbol{X}}_t = (\tilde{\boldsymbol{X}}_{1,t}, ..., \tilde{\boldsymbol{X}}_{n,t})'$, with $\tilde{\boldsymbol{X}}_{i,t} \in \mathbb{R}^p$ a sample of p-dimensional observations of the intra-evaluation-window factor returns. In other words, we incorporate the weight signal directly and proportionally in each of the asset returns.

Both portfolio returns and style factor returns are compounded over the risk evaluation interval for each simulation path, leading to $\tilde{\boldsymbol{y}}^h = (\tilde{y}_1^h, ..., \tilde{y}_n^h)'$ and $\tilde{\boldsymbol{X}} = (\tilde{\boldsymbol{X}}_1, ..., \tilde{\boldsymbol{X}}_n)'$ with $\tilde{\boldsymbol{X}}_i \in \mathbb{R}^p$ being a sample of p-dimensional simulated observations of the cumulative factor returns. For example, in the empirical application, we use the cumulative simulated h-period returns of a dynamic strategy that invests in each subperiod in each *separate* constituent of the Dow 30 index.

Since we repeat this procedure for n simulation paths, it follows by construction that these p prespecified synthetic factors combine the information on out-of-sample returns *and* daily changing weights.

3.2. Estimation of factor model

We maintain a linear relationship between multi-period portfolio return and our pre-specified synthetic factors (see Eq. (4)). However, the exposure vector $\boldsymbol{a}$ is typically unknown and has to be estimated. In low dimensions, the exposure vector is easily obtained using an ordinary least squares regression. Since the number of potential risk factors is large and/or some of the risk factors are highly linearly dependent (through, for example, a shared weight updating equation), it is important to regularize the influence of the factors. We recommend to use the elastic net regularization of Zou and Hastie (2005) to uniquely identify the vector of factor loadings.

The data matrix $\bar{\boldsymbol{X}}$ is the standardized version of the risk factor data matrix $\tilde{\boldsymbol{X}}$, with components $\bar{\boldsymbol{X}}_i = (\tilde{\boldsymbol{X}}_i - \text{av}_i)/\text{std}_i$, where av_i and std_i are the sample mean and standard deviation of $\tilde{\boldsymbol{X}}_i = (\tilde{X}_{i,1}, ..., \tilde{X}_{i,n})'$. The standardization is crucial in penalized regressions, since the penalty depends on the scale of the components.

To obtain the vector of slope coefficients, we minimize an objective function of the following form

$$\mathscr{L}(\bar{\boldsymbol{\alpha}},\bar{\boldsymbol{\beta}}) \quad = \quad \left\|\tilde{\boldsymbol{y}}^h - \left(\bar{\boldsymbol{\alpha}}+\bar{\boldsymbol{X}}\bar{\boldsymbol{\beta}}\right)\right\|_2^2 + \lambda\left[\frac{1}{2}(1-\gamma)\left\|\bar{\boldsymbol{\beta}}\right\|_2^2 + \gamma\left\|\bar{\boldsymbol{\beta}}\right\|_1\right], \tag{10}$$

in which $\|\cdot\|_\nu$ is the ℓ_ν norm and $\lambda \geq 0$ sets the level of regularization.[6]

We join prespecified factors and standardized errors together in the data matrix $\tilde{\boldsymbol{F}} \equiv (\tilde{\boldsymbol{X}}\ \tilde{\boldsymbol{e}})$. Similarly, slope coefficients and the standard deviation of the unexplained variation are combined in the exposure vector $\hat{\boldsymbol{a}} \equiv (\hat{\boldsymbol{\beta}}'\ \hat{\delta})' = (\hat{\beta}_1,...,\hat{\beta}_q,\hat{\delta})'$. Altogether, this leads to the following description of multi-period data-driven portfolio returns that are driven by factor returns: $\boldsymbol{y}^h = \hat{\boldsymbol{\alpha}} + \tilde{\boldsymbol{F}}\hat{\boldsymbol{a}}$, which now resembles Eq. (4).

3.3. Calculation of mean-variance-skewness-kurtosis risk

We estimate the mean vector, co-variance matrix, co-skewness matrix and co-kurtosis matrix of the data matrix $\tilde{\boldsymbol{F}}$ according to the formulas in Appendix A. The most straightforward way to estimate the co-moment matrices relies on the plug-in sample estimator. This approach is well-suited, since we rely on a large set of simulated observations to deal with the estimation variance of these estimators.

Having obtained the exposure vector $\boldsymbol{a}$ in the previous section, we estimate the multivariate downside risk functions $\rho(\hat{\boldsymbol{a}};\hat{\boldsymbol{\mu}},\hat{\boldsymbol{\Sigma}},\hat{\boldsymbol{\Phi}},\hat{\boldsymbol{\Psi}})$ that are closed form expressions of the portfolio composition and co-moments. As usual, we set a particular loss level (1% or 5%) and estimate downside risk. Finally, Euler's Theorem and the MVSK budgets are used to unravel aggregate portfolio risk into granular moment and factor risk budgets.

4. The unreliability of the square-root-of-time rule

In Figure 3 we use a simulated example to show the improvements of our SiMPA approach over the traditional square-root-of-time rule in the presence of dynamic weights.

Consider a monthly risk evaluation horizon with out-of-sample rebalancing points $t = 1,2,...,20$ and let asset $i = (1,2)$ make up a two-asset portfolio with asset returns drawn from a multivariate normal distribution. We consider a homogeneous asset mix in which we posit similar risk contributions, defined by a null mean vector and volatilities $(2.00,2.00)'$. Means and volatilities are expressed in percentages. For the sake of simplicity, the multivariate dependence parameter is set to zero. The portfolios start off with an equal allocation, $w_{i,t=0} = (0.5,0.5)'$.

The standard workhorse to assess multi-horizon risk is to scale risk estimates using the square-root-of-time rule. This approach embodies the buy-and-hold-assumption, which is implemented analytically by means of the true mean vector, the covariance matrix and the weights observed at the beginning of the risk evaluation horizon,

$$\boldsymbol{\mu} = \begin{pmatrix}0\\0\end{pmatrix}; \quad \boldsymbol{\Sigma} = \begin{pmatrix}.0004 & 0\\0 & .0004\end{pmatrix}; \quad \boldsymbol{w}_0 = \begin{pmatrix}.50\\.50\end{pmatrix}; \tag{11}$$

The key point that we stress in this paper is that it is indispensable to sort out the effects of dynamic weight adjustments when identifying the sources of multi-period risk. While this problem was pinpointed

Figure 3: Inaccuracy of square-root-of-time using one-month risk attribution

(a) Intra-month weight evolution

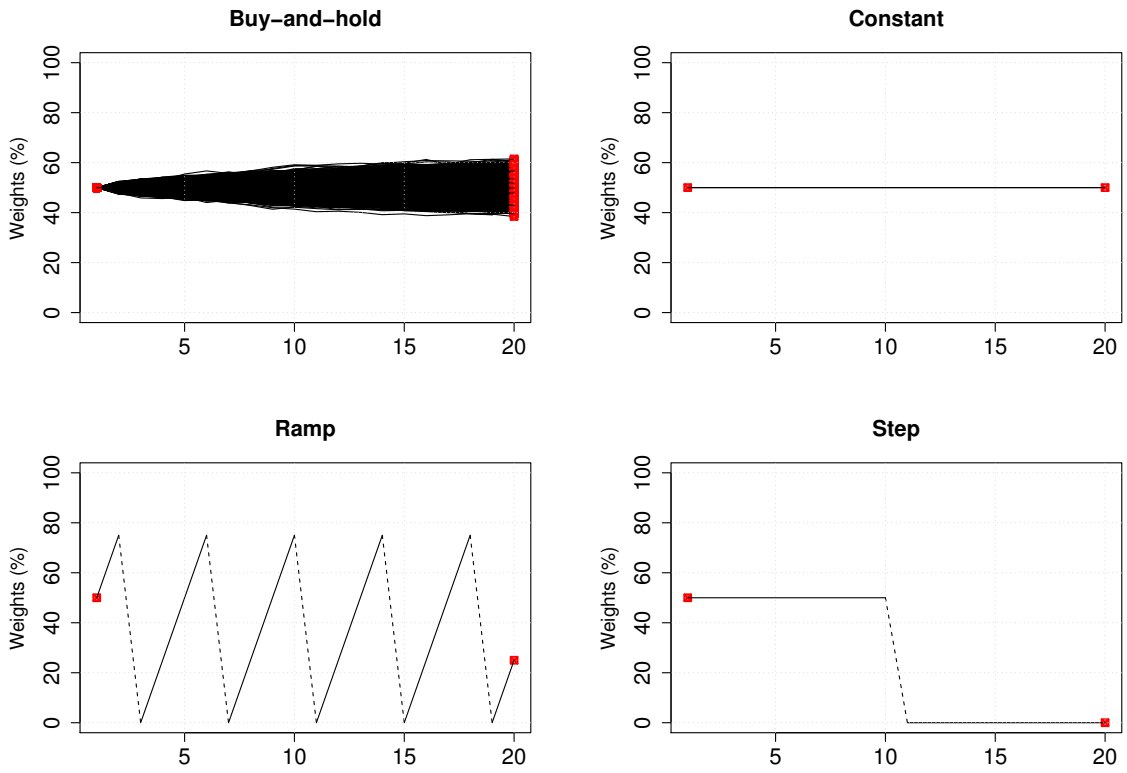

(b) Factor percentage decomposition of dynamic portfolios

Investment strategy Estimation strategy	- Square-root-of-time (1)	Buy-and-hold SiMPA (2)	Constant-Mix SiMPA (3)	Ramp SiMPA (4)	Step SiMPA (5)
Panel 1: *Average Risk factor allocation*					
Risk factor$_1$	–	0.992	0.994	0.994	0.993
Risk factor$_2$	–	0.989	0.991	0.990	0.987
Residual risk factor	–	0.003	0.003	0.004	0.005
Panel 2: *Average weekly standard deviation and contributions*					
Portfolio total	**6.325**	**6.248**	**6.237**	**7.391**	**7.650**
Risk factor$_1$	50.000	49.507	49.617	31.968	16.540
Risk factor$_2$	50.000	50.493	50.382	68.031	83.459
Residual risk factor	–	0.001	0.001	0.001	0.002

Note: In the top panel, we visualize weighting profiles for one iteration of $n = 10,000$ simulation paths of the weights across the risk evaluation horizon, consisting of a buy-and-hold strategy (top left), a constant process (top right), a ramp process (bottom left) and a step function (bottom right). In the bottom panel, we illustrate the inaccuracy of the square-root-of-time rule by decomposing the multi-period risk of a two-asset portfolio. We compare the analytical buy-and-hold assumption (square-root-of-time) with the four described deterministic weighting functions (using SiMPA), using 1,000 iterations and report the average. We report the multi-period exposure vector and percentage risk contributions for the portfolio standard deviation. Total risk (in bold) is reported as a risk number. The risk contributions are reported in percentages.

in Diebold et al. (1998), it is still unresolved in the context of risk allocation. In light of this problem, we consider the implications of four stylized weighting profiles on the evaluation of risk using the proposed SiMPA approach. The deterministic weight processes are defined as

$$\textbf{buy-and-hold:} \quad w_{1,t} = p_{1,t}/(p_{1,t}+p_{2,t}) \quad \text{with } p_{1,0}=p_{2,0}, \tag{12a}$$

$$\textbf{constant(-mix):} \quad w_{1,t} = 0.5, \tag{12b}$$

$$\textbf{ramp:} \quad w_{1,t} = \operatorname{mod}\big[(t+1)/4\big], \tag{12c}$$

$$\textbf{step:} \quad w_{1,t} = 0.5 - 0.5(t>2), \tag{12d}$$

in which $w_{1,t}$ indicates the capital to be invested in asset 1 at the intra-window time t and $\boldsymbol{p}_t = (p_{1,t}, p_{2,t})$ are the log asset prices recorded at time t. We assume a fully-invested portfolio. All processes, with the exception of the passive buy-and-hold strategy, are based solely on the time index t, and not the previous price path. The constant(-mix), step and ramp functions are chosen because of rapid changes, gradual changes and periods of constancy across the risk evaluation interval.

It is interesting to note the apparent resemblance of these patterns to actual practice in the financial industry. The constant-mix process is conceptually consistent with a balanced equally weighted portfolio. This strategy aims at diversification and, in doing so, downweighs winners and overweighs losers. The ramp profile mirrors a market timing strategy, which builds up capital steadily in a particular asset and disinvests after a distressing market signal. The step function appears like the flight-to-safety phenomenon, in which funds are suddenly shifted from an equally weighted portfolio to complete concentration in a safe haven asset.

In the utmost left column we report analytical results based on initial weights consistent with the buy-and-hold assumption. Absent any intra-window weight changes, the risk budgets behave as expected from their static portfolio composition and return characteristics. More precisely, in this setting, risk scaling characterizes a portfolio in which each component contributes equally to total portfolio risk. In columns (2) through (5), we apply the proposed SiMPA approach and use deterministic weight processes to replicate a dynamic investment strategy. SiMPA accounts for both the randomness in returns and randomness in weights and, thus, describes effective risk contributions.

We inspect the allocation of the exposure vector and the percentage risk contributions to portfolio volatility. The slope coefficients reported in panels (1) and (2) load on the transformed risk factors (associated to the corresponding assets) with a slope coefficient almost equal to 1. The residual risk factor is almost negligible. A similar multi-period allocation description is not possible for the square-root-of-time rule, since scaling does not have an obvious relation to the proposed active risk factor model.

The risk contributions in Panel 2 confirm the adequacy of the SiMPA approach. As expected, we observe that the SiMPA estimation strategy is able to capture the analytical buy-and-hold assumption (Column 1 vs. Column 2) with sufficient accuracy in terms of portfolio volatility and percentage factor contributions. The most remarkable aspect is the misclassification that results from the square-root-of-time rule. In particular, we observe that more frequent and/or abrupt movements lead to a misleading bias in percentage component contributions. The severest mismatch can be seen in the step function (Column 5), in which percentage contributions go from an expected 50/50 percentage risk budget judgement to an approximate 16/84 realized

attribution.

The results in this section confirm our intuition that the plain-vanilla square-root-of-time rule leads to misleading results in non-buy-and-hold settings. At minimum, our approach can be considered useful for assessing the validity and accuracy of the frequently assumed buy-and-hold investing strategy.

5. Empirical results

5.1. Data and strategy description

We study a representative data set composed of the Dow Jones Industrial Average constituents. The sample period is from March 17, 1987 to February 3, 2009 corresponding to 5,520 trading days and includes several episodes of exceptional risk (the LTCM collapse, the September 11 attacks, the dot-com bubble, the financial crisis of 07-08, etc.)[7] For the out-of-sample evaluations of a data-driven strategy in sections 5.2, we impose a minimum estimation window of length $T = 240$ days, starting from February 26, 1988. This sample window corresponds to 1,056 five-day risk evaluation windows, consisting of 5,280 potential rebalancing points at which the investment rule can change the portfolio composition.

Table 2 describes the variation in return distributions and non-normality in the observed financial returns across weekly risk management horizons. We report the averaged summary statistics by sectors for each of the constituents of the Dow index.

The companies belong to the following sectors: Energy (2), Financials (5), Industrials (6), Consumer Cyclicals (4), Technology (3), Computers & Technology (1), Healthcare (3), Consumer Non-Cyclicals, Telecom (2) and Oil & Gas (1). The number of assets operating under each sector label are reported in parentheses, and each ticker is reported in Column (2).

The data-driven investment algorithm that we investigate aims at floor protection by using a CPPI strategy. This means that the portfolio investment rule dynamically allocates capital between a risk-free fixed income asset (which provides protection against market losses) and a risky reference pool of assets (with upside potential). We refer to Black and Perold (1992) for a detailed treatment of portfolio insurance.

The weights on the asset returns at rebalancing date t are defined as

$$w_{i,t-1}^{\text{cppi}} = w_{i,t-1}^{\text{risky}} \frac{E_{t-1}}{V_{t-1}}, \tag{13}$$

in which $w_{i,t}^{\text{risky}}$ are the asset weights within the risky reference portfolio, the exposure $E_t = \max\{\min\{\pi C_t, V_t\}, 0\}$ is the nominal amount allocated to a risky portfolio of assets and V_t is the portfolio value, with $V_0 = 100$. This exposure is defined by the multiplier coefficient π and a cushion C_t. The latter indicates the difference between the portfolio value V_t and the constant floor $F = 90$ up to the portfolio's anniversary. The exposure is bounded to V_t so that no leverage is allowed. The floor level is yearly reset to avoid a cash lock-in.

The risky reference pool of assets is typically an index. We consider three types of prior-return-weighted portfolios that are rebalanced end-of-month: an equally weighted index, a low-risk index (computed via inverse volatility in the previous 240 trading days) and a price-weighted index. The application is chosen such that there are two types of dynamic weight adjustments within the risk evaluation horizon, namely,

Table 2: Full-sample summary statistics of weekly log-returns of Dow 30 constituents (grouped by sector)

Sector/Portfolio (1)	Tickers (2)	$\hat{\mu}_i(\%)$ (3)	$\hat{\sigma}_i(\%)$ (4)	$\hat{s}_i$ (5)	$\hat{k}_i$ (6)	$\min_i(\%)$ (7)	$\max_i(\%)$ (8)	$\text{mES}_i(\%)$ (9)
Panel 1: Dow 30 sectors								
Energy	AA, CVX	0.148	4.220	−0.756	5.815	−31.040	19.498	15.025
Financials	AXP, BAC, C, JPM, AIG	0.029	6.133	−4.254	99.090	−86.484	38.506	8.548
Industrials	BA, CAT, DD, GE, MMM, UTX	0.157	3.969	−0.609	7.046	−28.721	18.922	13.040
Consumer Cyclicals	DIS, GM, HD, MCD	0.140	4.672	−0.399	8.389	−35.427	28.391	8.677
Technology	HPQ, INTC, MSFT	0.279	5.354	−0.423	3.305	−34.666	21.035	14.919
Computers & Technology	IBM	0.122	4.111	−0.248	3.276	−25.196	17.173	10.820
Healthcare	JNJ, MRK, PFE	0.202	3.661	−0.272	2.487	−20.872	18.046	9.392
Consumer Non-Cyclicals	KO, PG, WMT	0.235	3.554	−0.720	7.047	−25.850	15.051	11.719
Telecom	T, VZ	0.154	3.648	−0.220	2.957	−24.118	16.137	9.259
Oil & Gas	XOM	0.243	2.908	−0.413	4.153	−21.110	14.503	8.273

Note: We report sector information and descriptive statistics for the in-sample weekly returns (non-annualized) of the constituents (grouped by sector) of the Dow 30 index. The full in-sample window spans the horizon March 17, 1987 to February 3, 2009. We report the Sector/Portfolio (Column 1), the corresponding tickers (Column 2), the respective values for mean (Column 3), standard deviation (Column 4), skewness (Column 5), excess kurtosis (Column 6), minimum percentage (Column 7), maximum percentage (Column 8) and modified expected shortfall (Column 9).

(i) a prior-return-weighted monthly rebalancing in the reference indices and (ii) a dynamic floor-protection which allocates funds to the reference portfolio on a daily basis.

Table 3 describes the variation in return distributions and non-normality in the observed financial returns across weekly risk management horizons of the prior-return-weighted indices (Panel 1) and the corresponding CPPI-rebalanced portfolios (Panel 2).

Unsurprisingly, for low values of the multiplier, the standard deviations (Column 4), minima (Column 7), maxima (Column 8) and modified expected shortfall (Column 9) are considerably lower compared to the assets and Dow 30 indices (cfr. Table 2). Note that when the multiplier increases the CPPI portfolio returns become increasingly similar to the equity index returns. Hence, the choice of multiplier thus determines the trade-off of a reward vs. risk.

The values for skewness (Column 5) and excess kurtosis (Column 6) are in all cases high enough to reject the p-value of the Jarque-Bera statistic for normality at less than 1% (not tabulated). Because of the non-normality of these returns, they constitute an excellent case for advocating the use of MVSK portfolio risk measures. Note that these strategies deliberately affect the portfolio moments through floor protection (as they cover the left tail and aim for high upside potential).

In Figure 4 we graph the effect of floor-protection on the performance and weights of an actively-managed, equally weighted Dow 30 index.

In the top panel, we observe that the investment algorithm leads to more concentrated returns as compared to the risky asset mix, indicative of the lower standard deviation and dampened minima-maxima range. More interestingly, the bottom panel contains a visual depiction of the typical sharp and abrupt movements in allocation for a strategy with year-end resets. The fluctuations of the portfolio weights summarize the history of the CPPI's exposure to the equally weighted index. In the allocation view of Figure 4, we observe

Table 3: Full-sample summary statistics of weekly log-returns of active portfolios on Dow 30 constituents

Portfolio	$\hat{\mu}_i(\%)$	$\hat{\sigma}_i(\%)$	$\hat{s}_i$	$\hat{k}_i$	$\min_i(\%)$	$\max_i(\%)$	$\mathrm{mES}_i(\%)$
(1)	(2)	(3)	(4)	(5)	(6)	(7)	(8)
Panel 1: Prior-return-weighted Dow 30 indices							
Equally weighted	0.254	2.592	−0.555	5.375	−17.448	13.071	8.060
Low-risk	0.251	2.161	−0.469	4.600	−12.637	12.080	6.307
Price-weighted	0.259	2.769	−0.328	3.652	−15.608	12.649	7.453
Panel 2: CPPI portfolios							
2a: Reference index: Equally weighted index							
CPPI ($\pi = 2$)	0.054	0.526	−0.465	2.648	−3.284	2.125	1.405
CPPI ($\pi = 4$)	0.122	1.158	−0.334	3.435	−7.425	5.982	3.084
CPPI ($\pi = 6$)	0.171	1.597	−0.535	4.532	−11.136	6.606	4.776
CPPI ($\pi = 8$)	0.188	1.797	−0.780	6.104	−14.680	7.089	6.149
CPPI ($\pi = 10$)	0.197	1.934	−1.459	15.124	−21.390	8.495	9.230
2b: Reference index: Low-risk index							
CPPI ($\pi = 2$)	0.052	0.460	−0.586	4.055	−3.284	1.729	1.365
CPPI ($\pi = 4$)	0.112	1.011	−0.456	4.792	−7.425	4.849	2.959
CPPI ($\pi = 6$)	0.157	1.441	−0.687	6.188	−11.136	5.587	4.797
CPPI ($\pi = 8$)	0.173	1.621	−0.938	8.509	−14.680	5.587	6.208
CPPI ($\pi = 10$)	0.175	1.757	−1.866	21.763	−21.390	5.587	8.732
2c: Reference index: Price-weighted index							
CPPI ($\pi = 2$)	0.059	0.586	−0.242	3.398	−3.419	2.843	1.503
CPPI ($\pi = 4$)	0.138	1.324	−0.195	5.868	−9.616	7.239	3.436
CPPI ($\pi = 6$)	0.182	1.739	−0.161	5.766	−11.167	10.944	4.412
CPPI ($\pi = 8$)	0.190	1.929	−0.426	6.384	−14.752	11.075	5.777
CPPI ($\pi = 10$)	0.188	2.081	−1.131	13.436	−21.850	11.075	8.845

Note: We report descriptive statistics for the in-sample weekly returns (non-annualized) of the monthly-rebalanced indices of the Dow 30 index (an equally weighted index, a low-risk index and a price-weighted index) and daily-rebalanced CPPI portfolios (with multipliers $\pi = 2, 4, 6, 8, 10$). The full in-sample window spans the horizon March 17, 1987 to February 3, 2009. We report the Portfolio (Column 1) the respective values for mean (Column 2), standard deviation (Column 3), skewness (Column 4), excess kurtosis (Column 5), minimum percentage (Column 6), maximum percentage (Column 7) and modified expected shortfall (Column 8).

that across 1987–1999 the investment strategy was strongly invested in the market, showing many spikes in exposure to the risky reference portfolio. The flat lines correspond to the bounded portfolio value. As of 2000, we observe more turbulence in the strategy. We see that the allocation strongly moves away from the boundaries of 0 and 100 percent. Needless to say, such large swings in the composition can have a significant impact on the operations of the investor in gauging the risk at longer horizons. The portfolio at the beginning of the risk evaluation interval shares little relation to the variety of positions that could be taken in the course of the next few days. imilarly

5.2. Diagnostic sector risk budgeting of CPPI Dow 30 portfolios

In this subsection, we show the usefulness of a two-dimensional risk decomposition for the CPPI investor using a one-week risk evaluation horizon. We focus on concentration risk and the risk-return trade-off.

In order to gauge risk over the weekly risk evaluation intervals, we rely on Boudt et al. (2008)'s modified expected shortfall (mES) as a risk measure, which is of the form proposed in Eqs. (8a) – (8e). This risk measure accounts for the asymmetry and the peakedness of the portfolio return distribution.

We take an ex-ante approach and simulate asset returns for each out-of-sample day. We rely on the

Figure 4: The effect of daily floor-protection on the weights and performance of a CPPI invested in the equally weighted Dow 30 index

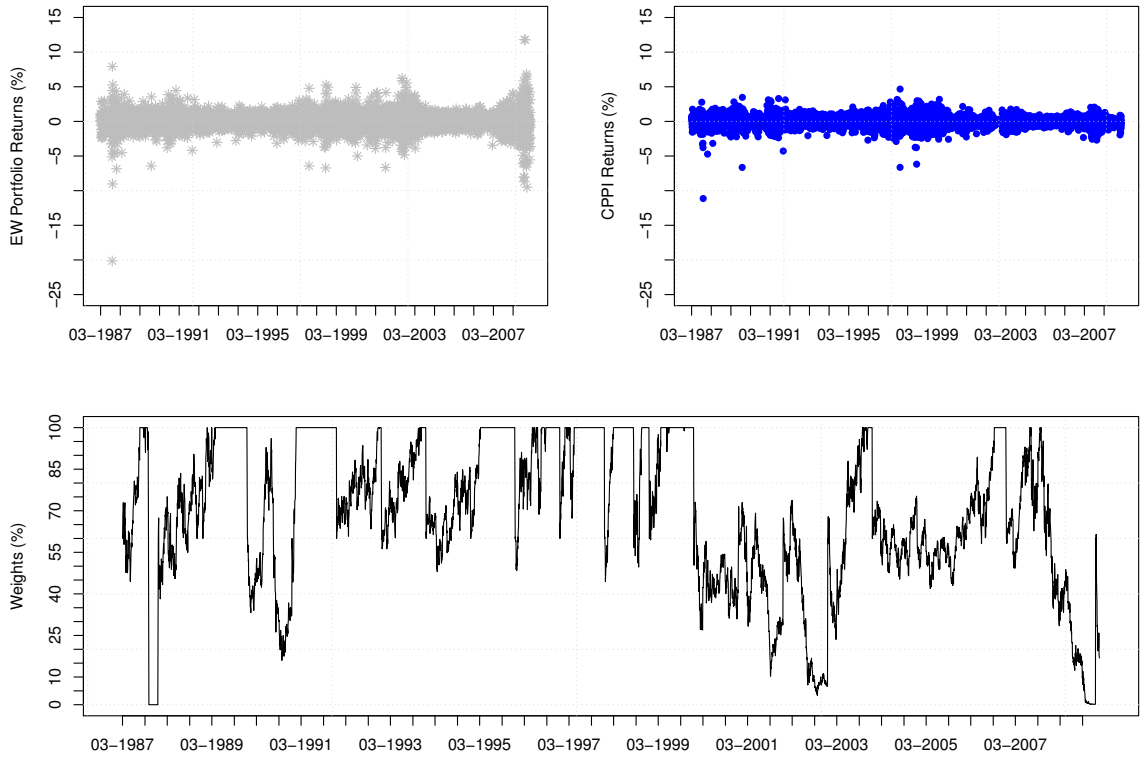

Note: We plot in-sample rebalancing results of a CPPI strategy (multiplier $\pi = 6$) on daily equally weighted (EW) Dow 30 index returns (risky reference portfolio). The full in-sample window spans the horizon March 17, 1987 to February 3, 2009, consisting of $5,520$ observations. We graph the weights signalled by the CPPI strategy to be invested in the risky reference index (top), daily returns of an equally weighted Dow 30 portfolio (bottom-left) and CPPI-rebalanced returns (bottom-right).

Conditionally Heteroscedastic Independent Components Analysis Generalized Orthogonal (CHICAGO) GARCH model of Broda and Paolella (2009) to model the temporal dependence up to the fourth-order moment of the multivariate asset return series, as detailed in Appendix C. The simulated out-of-sample asset return distribution consists of 500 draws for each day in the five-step prediction interval. The model for the asset returns is re-estimated using all the data up to that point in time.

Table 4 provides a direct view of concentration risk in floor-protected portfolios using the proposed companion table. The estimators – averaged across 1,056 risk evaluation horizons – cover the average five-day risk of active CPPI fluctuations over the period 1988-2009. Emphasis is placed on percentage sector-budgets, meaning that the budgets sum to 100 percent. The last column represents the position size with respect to these factors.

We observe similar levels of portfolio expected shortfall across the three CPPI portfolios (3.578, 3.937 and 3.616 percent, respectively), rendering these portfolios observationally equivalent using univariate tools. A meaningful practice of risk assessment recognizes that these similar levels of portfolio risk are caused by

Table 4: Sector-risk percentage risk allocation

	Modified expected shortfall perc. contributions (%)					
	Mean (1)	St.Dev. (2)	Skew (3)	Kurtosis (4)	Total (5)	Avg. alloc. (6)
Panel 1: CPPI with equally weighted index (3.499%)						
Energy (%)	−0.787	11.445	−0.720	0.147	10.085	7.077
Financials (%)	−0.990	7.190	−0.341	−0.099	5.760	9.024
Industrials (%)	−2.556	34.378	−2.234	0.057	29.646	23.768
Consumer Cyclicals (%)	−1.448	16.878	−1.101	0.054	14.383	14.534
Technology (%)	−1.208	9.364	−0.427	−0.026	7.703	10.500
Computers & Technology (%)	−0.562	3.395	−0.228	−0.036	2.569	4.069
Healthcare (%)	−1.254	14.470	−0.983	0.064	12.296	10.011
Consumer Non-Cyclicals (%)	−0.903	6.698	−0.324	−0.093	5.377	8.058
Telecom (%)	−1.129	11.186	−0.519	0.092	9.629	8.872
Oil & Gas (%)	−0.387	3.100	−0.145	−0.017	2.552	4.083
Residual (%)	0.000	0.001	0.001	0.000	0.001	0.004
Total	−11.226	118.105	−7.021	0.142	**100.000**	**100.000**
Panel 2: CPPI with low-risk index (3.967%)						
Energy (%)	−0.767	12.891	−0.944	0.022	11.202	8.265
Financials (%)	−1.016	7.803	−0.681	0.118	6.224	11.416
Industrials (%)	−2.591	35.037	−4.456	14.578	42.568	24.206
Consumer Cyclicals (%)	−0.633	7.939	−0.672	−0.504	6.129	7.771
Technology (%)	−0.040	0.326	−0.032	0.009	0.263	0.525
Computers & Technology (%)	−0.456	3.380	−0.318	−0.160	2.446	4.142
Healthcare (%)	−1.113	13.982	1.033	−6.531	7.370	10.491
Consumer Non-Cyclicals (%)	−1.421	13.665	4.578	−11.510	5.313	14.319
Telecom (%)	−1.326	13.304	−0.773	0.096	11.302	11.033
Oil & Gas (%)	−0.801	8.437	−0.468	0.005	7.173	7.822
Residual (%)	0.000	0.001	−0.001	0.011	0.010	0.010
Total	−10.164	116.765	−2.735	−3.866	**100.000**	**100.000**
Panel 3: CPPI with price-weighted index (3.517%)						
Energy (%)	−0.410	5.651	−0.422	0.159	4.978	3.794
Financials (%)	−0.675	4.861	−0.051	−0.040	4.095	5.995
Industrials (%)	−1.575	21.021	−3.156	1.156	17.446	16.593
Consumer Cyclicals (%)	−2.112	27.097	−2.651	0.577	22.911	43.784
Technology (%)	−3.256	36.334	4.195	−3.153	34.120	6.564
Computers & Technology (%)	−0.216	1.070	−0.172	0.017	0.699	3.952
Healthcare (%)	−0.858	7.870	−0.362	0.138	6.788	5.241
Consumer Non-Cyclicals (%)	−0.866	5.427	1.413	−0.594	5.380	5.258
Telecom (%)	−0.652	6.655	−7.481	3.133	1.654	5.869
Oil & Gas (%)	−0.259	1.835	0.576	−0.225	1.927	2.948
Residual (%)	0.000	0.001	0.000	0.001	0.002	0.003
Total	−10.879	117.820	−8.110	1.169	**100.000**	**100.000**

Note: We report average sector/moment percentage risk contributions to total modified expected shortfall for three CPPI portfolios; equally weighted (Panel 1), low-risk (Panel 2) and price-weighted index portfolio (Panel 3). The out-of-sample window spans the horizon February 26, 1988 to March 3, 2009. The total risk levels are reported in the headings of each panel. For each index, we report the risk budgeting table, consisting of the percentage mean contribution to risk (Column 1), the percentage volatility contribution to risk (Column 2), the percentage skewness contribution to risk (Column 3), the percentage kurtosis contribution to risk (Column 4), the total modified expected shortfall (Column 5) and the average exposure vector (Column 6). Each column contribution is made up of sector contributions. For each portfolio budget, we highlight the largest relative positive contributor and, in lightgray, the two subsequent highest contributors.

different drivers of downside risk.

In the bottom rows, we observe that the portfolios have meaningful non-Gaussian attributes. Indeed, for all the indices, the portfolio expected shortfall is affected by a moderately negative percentage skewness contribution (Column 3), meaning that skewness of the out-of-sample distribution, on average, lowers modified expected shortfall estimates. This is different from kurtosis contribution to expected shortfall, in which the portfolio percentage kurtosis-contribution is practically negligible (Column 4).

To help understand what drives these portfolio-level mean, variance, skewness and kurtosis budgets, we rely on factor attribution analysis, offering us a picture where risk is coming from. We shade the three most likely ex-ante hot spots that merit the investor's attention. Despite the fact that these index portfolios contain the same Dow 30 constituents, we clearly recover a different structure of risk contributions under different investment strategies. The low-risk CPPI portfolio, seems to shy away from Technology and Computers & Technology. The diagnostic table also points toward an excessive kurtosis contribution in the Industrials category. In the price-weighted Dow 30 index we find a different factor mix: the highest contributor is now the Technology sector. These results show that it is possible to mix weight processes, while still distinguishing between factor and moment contributions, which is of course essential from a diversification perspective.

Once we have identified the hot spots, the next step in managing portfolio risk is to decide how to change the composition. An additional advantage of our approach is that it yields both performance (proxied by mean contributions) and risk contributions. It is insightful to jointly consider them in a scatter plot reporting the performance contribution to risk on the vertical axis and the factor risk contributions on the horizontal axis. In case the portfolio achieves the highest relative performance, as is defined by the ratio between portfolio performance and portfolio risk, all dots are on a line with a slope equal to the relative performance of the portfolio (see e.g., Ardia et al., 2018). Components that are above (resp. below) the line contribute relatively more (resp. less) to performance than to risk. We show this performance-risk allocation chart in Figure 5.

The relative performance of the portfolio can be marginally improved by decreasing (resp. increasing) the allocation to a position below (resp. above) the line. For example, we observe the largest absolute deviation from maximum relative performance in the low-risk CPPI portfolio. Industrials stand out as an obvious candidate for attention: the sector contributes a substantial portion to risk without a corresponding contribution to performance. As is clear in Table 4, the Industrials sector also has a significant overweight position, partly explaining the excessive risk contribution. It is likely that lowering the exposure, at least at the margin, will reduce risk and improve the relative performance.

Figure 5: Average performance-risk contributions of a CPPI invested in prior-return-weighted Dow 30 indices

(a) Equally weighted index

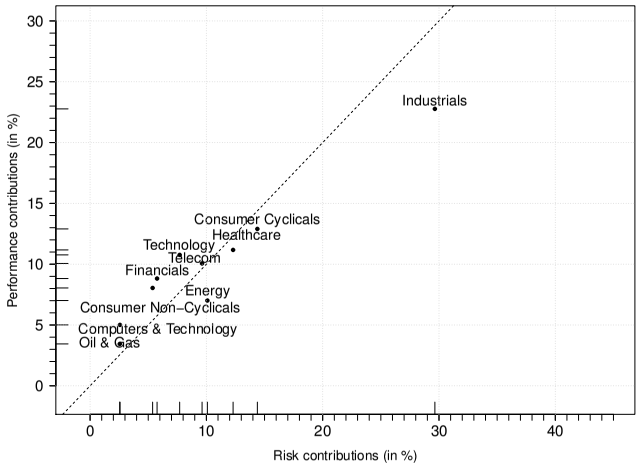

(b) Low-risk index

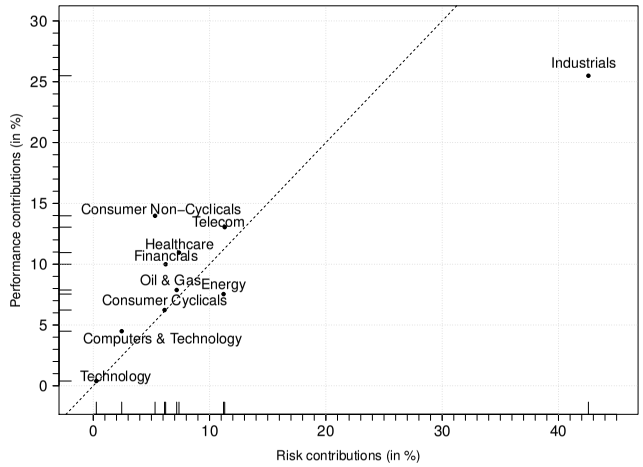

(c) Price index

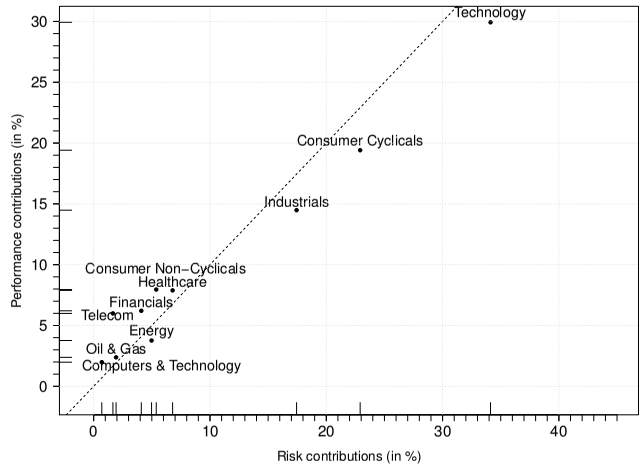

Note: We plot the performance-risk allocation chart for the different CPPI portfolios under consideration (i.e. equally weighted, low-risk and price). The vertical axis shows the performance contribution to risk (proxied by mean contributions) and the horizontal axis shows the factor risk contributions of each of the sectors. The slope of the line indicates the maximum relative performance, as defined by the ratio between portfolio performance and portfolio risk.

6. Concluding remarks

Sophisticated algorithmic techniques are complementing human judgement across the fund industry. Nonetheless, asset class strategists, risk managers, or anyone who gauges the performance of the investment strategy on an intermittent basis, rarely acknowledges the feature that the composition tends to change regularly, both within and across days.

To address the variability within the risk evaluation horizon, we propose a solution for investments with data-driven portfolio weights that may change within the risk evaluation horizon. The approach uses simulations from a flexible risk factor model that accommodates these weight dynamics directly within the covariates. As a result, we are able to compute risk contributions for horizons longer than the frequency at which portfolios are rebalanced. To aid in investment judgement, we cast multi-period portfolio risk into a mean-variance-skewness-kurtosis format accounting for the longer-horizon structural relationship between the underlying assets in a data-driven investment strategy.

We illustrate the usefulness of the novel framework in two applications. First, we confirm our intuition that the plain-vanilla square-root-of-time rule leads to misleading results in non-buy-and-hold settings. Second, an out-of-sample study provides evidence that by looking *inside* the portfolio, the patterns in granular *contributions* to portfolio risk might now be used to make more informed decisions on the investment process of CPPI portfolios.

Notes

[1] See for example, CFA institute, 2019; AI pioneers in investment management; Economist, October 2019; The stockmarket is now run by computers, algorithms and passive managers; Financial Times, October 2019, Meet The Buffet bot: quant funds try to crack the value code; Financial Times, July 2019, Quants seek human touch in reboot of investing strategy; Financial Times, October 2019, Why hedge fund managers are happy to let the machines take over; Financial Times, October 2019, Will bots replace humans in active equity investment

[2]Examples include Candriam Dynamic Global, KBC Privileged Portfolio Pro (95, 90 and 85), BNP Paribas B Control, DWS Fund Global Protect (80 and 90), Swiss Life Multi Asset Protected Fund 80 and Fideuram Equity Smart Beta Dynamic Pro 80.

[3]We denote $\boldsymbol{\Psi}^*$ as the co-kurtosis matrix. The matrix $\boldsymbol{\Psi}_{\mathscr{N}}$ is the co-kurtosis matrix under multivariate normality. For example, for dimensions equal to 2, we have that the bivariate normal co-skewness matrix $\boldsymbol{\Phi}_{\mathscr{N}}$ and co-kurtosis matrix $\boldsymbol{\Psi}_{\mathscr{N}}$ are equal to,

$$\boldsymbol{\Phi}_{\mathscr{N}} = \begin{bmatrix} 0 & 0 & 0 & 0 \\ 0 & 0 & 0 & 0 \end{bmatrix} \quad \text{and} \quad \boldsymbol{\Psi}_{\mathscr{N}} = \begin{bmatrix} 3 & 0 & 0 & 1 & 0 & 1 & 1 & 0 \\ 0 & 1 & 1 & 0 & 1 & 0 & 0 & 3 \end{bmatrix}. \tag{14}$$

Such that $\boldsymbol{\Psi} = \boldsymbol{\Psi}^* - \boldsymbol{\Psi}_{\mathscr{N}}$ can be interpreted as the excess co-kurtosis matrix.

[4] Homogeneity of degree one or, equivalently, multiplicative scaling behaviour, indicates that if the exposure vector is $\boldsymbol{a}$ multiplied by a positive scalar e, these risk measures are also scaled by the same scalar: $\rho(e\boldsymbol{a}) = e\rho(\boldsymbol{a})$.

[5] Andreas Steiner. Tail risk attribution. Unpublished results.

[6] The implementation of the elastic net regularization in Eq. (10) requires the calibration of the penalty parameters λ and γ. We follow the idea of Zou et al. (2007) and minimize a BIC-like criterion (where BIC stands for Bayesian Information Criterion) over a grid of (λ, γ) candidate pairs. The standard deviation δ of the unexplained variation is calculated in accordance with Reid et al. (2016).

[7] The daily log-returns are available in the R package **rmgarch** (Ghalanos, 2019).

APPENDIX

A. Multivariate factor co-moments and partial derivatives

The multivariate factor co-moments used in Section 2.2 are defined as

$$\begin{aligned}
\boldsymbol{\Sigma} &= \mathbb{E}\left[(\boldsymbol{f}-\boldsymbol{\mu})(\boldsymbol{f}-\boldsymbol{\mu})'\right] && \text{(15a)}\\
\boldsymbol{\Phi} &= \mathbb{E}\left[(\boldsymbol{f}-\boldsymbol{\mu})(\boldsymbol{f}-\boldsymbol{\mu})'\otimes(\boldsymbol{f}-\boldsymbol{\mu})'\right] && \text{(15b)}\\
\boldsymbol{\Psi}^{*} &= \mathbb{E}\left[(\boldsymbol{f}-\boldsymbol{\mu})(\boldsymbol{f}-\boldsymbol{\mu})'\otimes(\boldsymbol{f}-\boldsymbol{\mu})'(\boldsymbol{f}-\boldsymbol{\mu})'\right], && \text{(15c)}
\end{aligned}$$

in which $\boldsymbol{f}$ denotes the q-dimensional of multi-period risk factor returns, $\boldsymbol{\mu}$ is the vector of factor means and $\otimes$ denotes the Kronecker product. Then, for a given exposure vector $\boldsymbol{a}$, the second- to fourth-order moments of the portfolio return are defined as

$$\begin{aligned}
m_2 &= \boldsymbol{a}'\boldsymbol{\Sigma}\boldsymbol{a} && \text{(16a)}\\
m_3 &= \boldsymbol{a}'\boldsymbol{\Phi}(\boldsymbol{a}\otimes\boldsymbol{a}) && \text{(16b)}\\
m_4 &= \boldsymbol{a}'\boldsymbol{\Psi}^{*}(\boldsymbol{a}\otimes\boldsymbol{a}\otimes\boldsymbol{a}). && \text{(16c)}
\end{aligned}$$

Portfolio skewness s and excess portfolio kurtosis k are given by

$$\begin{aligned}
s &= m_3/\left(m_2\right)^{3/2} && \text{(17a)}\\
k &= m_4/m_2^2-3. && \text{(17b)}
\end{aligned}$$

For a given portfolio exposure vector $\boldsymbol{a}$, the partial derivatives to component $j=(1,...,q)$ of the second- to fourth-order moments of the portfolio return are defined as

$$\begin{aligned}
\partial_j m_2 &= 2\left[\boldsymbol{\Sigma}\boldsymbol{a}\right]_j && \text{(18a)}\\
\partial_j m_3 &= 3\left[(\boldsymbol{\Phi}(\boldsymbol{a}\otimes\boldsymbol{a})\right]_j && \text{(18b)}\\
\partial_j m_4 &= 4\left[(\boldsymbol{\Psi}^{*}(\boldsymbol{a}\otimes\boldsymbol{a}\otimes\boldsymbol{a})\right]_j. && \text{(18c)}
\end{aligned}$$

The corresponding partial derivatives of the portfolio skewness s and excess portfolio kurtosis k are given by

$$\begin{aligned}
\partial_j s &= (2m_2^{3/2}\partial_i m_3 - 3m_3 m_2^{1/2}\partial_j m_2)/2m_2^3 && \text{(19a)}\\
\partial_j k &= (m_2\partial_j m_2 - 2m_4\partial_i m_2)/m_2^3. && \text{(19b)}
\end{aligned}$$

B. Mean-variance-skewness-kurtosis risk functions

Let y^h be a random variable of portfolio h-period returns. It is convenient to break down the complete characterization of y^h into the conditional mean and the conditional variance containing the scale parameters and shape parameters that determine the form of a conditional family of distributions. The quantities of

interest in this article are risk functions $\rho(\boldsymbol{a};\boldsymbol{\mu},\boldsymbol{\Sigma},\boldsymbol{\Phi},\boldsymbol{\Psi})$ that depend on: (i) a linear description of the univariate random variable in terms of risk factors, and (ii) the risk factor co-moments.

The class of risk functions consists of density and quantile expressions and are typically expressed for the random variable Z with mean zero and unit variance. We may write that the standardized innovations Z follow a conditional distribution g with vector of shape parameters $\boldsymbol{\eta}$, $Z \sim g(Z|\boldsymbol{\eta})$. The shape parameter $\boldsymbol{\eta}$ of the conditional distribution involves parameters that capture the asymmetry and fat-tailedness of the distribution.

When it is believed that the true *pdf* of the random variable Z is rather close to a normal one, most expansions of the density are based on the form

$$g(Z|\boldsymbol{\eta}) = \varphi(Z)\, p_d(Z|\boldsymbol{\eta}), \tag{20}$$

where $\varphi(Z)$ is the density of a standard normal random variable and the function p_d, a polynomial of degree d, is such that the first moments of Z are equal to the moments of the approximating $g(Z|\boldsymbol{\eta})$. For example, the Edgeworth expansion is a typical representation of this form,

$$p_6(Z|\boldsymbol{\eta}) = 1 + \frac{\gamma_1}{6}H_3(Z) + \frac{\gamma_2}{24}H_4(Z) + \frac{\gamma_1^2}{72}H_6(Z), \tag{21}$$

in which H_v denotes the vth Hermite polynomial and $\boldsymbol{\eta} = (\gamma_1, \gamma_2)'$. It can be shown that the two parameters γ_1 and γ_2 are directly related to the skewness s and excess kurtosis k of $g(Z|\boldsymbol{\eta})$.

Quantile approximations are also popular in the literature. The Cornish-Fisher equation is based on inverting Eq. (20), in cumulative form, to obtain, for a level $\theta \in (0,1)$

$$G_r^{-1}(\theta) = z_\theta + \sum_{l=1}^{r} P_l(z_\theta), \tag{22}$$

with z_θ the Gaussian quantile function.

Using previously mentioned insights, Zangari (1996) defines the θ% modified value-at-risk as

$$\mathrm{mVaR}_\theta(\boldsymbol{a};\boldsymbol{\mu},\boldsymbol{\Sigma},\boldsymbol{\Phi},\boldsymbol{\Psi}) \;=\; -\boldsymbol{a}'\boldsymbol{\mu} - \sigma g_\theta, \tag{23}$$

with $g_\alpha = G_2^{-1}(\theta)$ the second-order Cornish-Fisher expansion around the Gaussian quantile function and $\sigma = \sqrt{m_2}$ being the univariate portfolio volatility. Similarly, Boudt et al. (2008) and Martin and Arora (2017) define θ% modified expected shortfall as

$$\mathrm{mES}_\theta(\boldsymbol{a};\boldsymbol{\mu},\boldsymbol{\Sigma},\boldsymbol{\Phi},\boldsymbol{\Psi}) \;=\; -\boldsymbol{a}'\boldsymbol{\mu} + \sqrt{m_2}\, E_{G_2}[Z\,|\,Z \le g_\theta], \quad \text{with}\, g_\theta = G_2^{-1}(\theta), \tag{24}$$

with

$$E_{G_2}[Z\,|\,Z \le g_\theta] = \frac{1}{\theta}\left\{\phi(g_\theta)\Big[1 + \frac{1}{6}g_\theta^3 s + \frac{1}{72}(g_\theta^6 - 9g_\theta^4 + 9g_\theta^2 + 3)s^2 + \frac{1}{24}(g_\theta^4 - 2g_\theta^2 - 1)k\Big]\right\}.$$

This equation involves the density of the Cornish-Fisher quantile $\phi(g_\theta)$ and powers of the same quantile function g_θ.

C. CHICAGO model of Broda and Paolella (2009)

In this paper, we rely on an extension of the Generalized Orthogonal GARCH (or GO-GARCH) model proposed by Van der Weide (2002) to model observed asset return series into an independent factor framework that provides a feasible model for large-dimensional multivariate modelling of asset returns. The most important characteristic is that the feasibility of the approach is based on an independent factor representation which separates the estimation of the correlation structure from the univariate dynamics and, thus, allows for the incorporation of nonnormal innovations. Moreover, this approach is extremely flexible as the corresponding Generalized Hyperbolic distribution nests, among others, the Normal, Student t and Laplace.

Consider the random vector $\boldsymbol{r}_t = (r_{1,t}, ..., r_{n,t})'$, with $\mathbb{E}[\boldsymbol{r}_t|\mathscr{F}_{t-1}] = \boldsymbol{\mu}_t$ being the $(n,1)$ vector of conditional asset means and $\mathscr{F}_{t-1}$ being the information set consisting of past realizations $\boldsymbol{r}_t$. The GO-GARCH model then maps innovations, $\boldsymbol{u}_t = \boldsymbol{r}_t - \boldsymbol{\mu}_t$, onto an unobserved independent factor framework. The joint dynamics are given by

$$\boldsymbol{r}_t|\mathscr{F}_{t-1} = \boldsymbol{\mu}_t + \boldsymbol{u}_t \tag{25a}$$

$$\boldsymbol{u}_t = \boldsymbol{A}\boldsymbol{\Lambda}_t \tag{25b}$$

in which the innovation vector $\boldsymbol{u}_t$ is model as a linear combination of d unobserved factors $\boldsymbol{\Lambda}_t$ or so-called structural errors, $\boldsymbol{A}$ is an time-invariant, invertible mixing matrix. The authors impose the identifying condition that factors are assumed to be independent and have unit variance. Via a polar decomposition, matrix $\boldsymbol{A}$ is factorized into a symmetric, de-whitened square root of the unconditional covariance matrix $\boldsymbol{\Sigma}^{1/2}$ and an orthogonal rotation matrix $\boldsymbol{U}$:

$$\boldsymbol{A} = \boldsymbol{\Sigma}^{1/2}\boldsymbol{U}. \tag{26}$$

The mixing matrix therefore represents the independent factor weights assigned to each asset. The factors have a GARCH-type dynamics.

Originally, this model was estimated via a 1-step maximum likelihood approach to jointly estimate the rotation matrix and factor dynamics. Differently, in the Conditionally Heteroscedastic Independent Components Analysis Generalized Orthogonal (CHICAGO) GARCH model of Broda and Paolella (2009), the authors propose a two-step approach which exploits the decomposition in Eq. (26). The unconditional covariance matrix is obtained from the ordinary least squares residuals, the matrix $\boldsymbol{U}$ is estimated in a separate step by means of Independent Component Analysis (ICA), which allow univariate factor dynamics and the innovations distribution to be estimated separately from the covariance specification. The factor dynamics conditionally follow the multivariate affine Generalized Hyperbolic (maGH) distribution of Schmidt et al. (2006), in which each component is expressed as a linear combination of independent univariate General Hyperbolic variables. These independent margins that allow to take separate values of skewness and kurtosis. Note that the factor dynamics have non-time varying higher moments within the Generalized Hyperbolic

distribution. For further elaboration on the model interpretation and fitting routine, we refer to Boudt et al. (2019). For a practical implementation, we refer to the R package **rmgarch** (Ghalanos, 2019).

References

Ardia, D., Boudt, K., and Nguyen, G. (2018). Beyond risk-based portfolios: balancing performance and risk contributions in asset allocation. Quantitative Finance, 18(8):1249–1259.

Ardia, D., Boudt, K., and Wauters, M. (2016). Smart beta and CPPI performance. Finance, 37(3):31–65.

Baştürk, N., Borowska, A., Grassi, S., Hoogerheide, L., and van Dijk, H. K. (2019). Forecast density combinations of dynamic models and data driven portfolio strategies. Journal of Econometrics, 210(1):170–186.

Black, F. and Perold, A. F. (1992). Theory of constant proportion portfolio insurance. Journal of Economic Dynamics and Control, 16(3-4):403–426.

Boudt, K., Cornilly, D., and Verdonck, T. (2020a). A coskewness shrinkage approach for estimating the skewness of linear combinations of random variables. Journal of Financial Econometrics, 18(1):1–23.

Boudt, K., Cornilly, D., and Verdonck, T. (2020b). Nearest comoment estimation with unobserved factors. Journal of Econometrics (In Press).

Boudt, K., Galanos, A., Payseur, S., and Zivot, E. (2019). Multivariate GARCH models for large-scale applications: A survey. In Vincod, H. D. and Rao, C. R., editors, Handbook of Statistics, Volume 41.

Boudt, K., Peterson, B. G., and Croux, C. (2008). Estimation and decomposition of downside risk for portfolios with non-normal returns. Journal of Risk, 11(2):79–103.

Broda, S. A. and Paolella, M. S. (2009). CHICAGO: A fast and accurate method for portfolio risk calculation. Journal of Financial Econometrics, 7(4):412–436.

Connor, G. (1995). The three types of factor models: A comparison of their explanatory power. Financial Analysts Journal, 51(3):42–46.

De Prado, M. L. (2018). Advances in Financial Machine Learning. John Wiley & Sons.

Diebold, F. X., Hickman, A., Inoue, A., and Schuermann, T. (1998). Scale models. Risk, 11:104–107.

Francq, C. and Zakoïan, J.-M. (2018). Estimation risk for the VaR of portfolios driven by semi-parametric multivariate models. Journal of Econometrics, 205(2):381–401.

Fung, W. and Hsieh, D. A. (2001). The risk in hedge fund strategies: Theory and evidence from trend followers. Review of Financial studies, 14(2):313–341.

Ghalanos, A. (2019). rmgarch: Multivariate GARCH models. R package version 1.3-7.

Gourieroux, C., Laurent, J.-P., and Scaillet, O. (2000). Sensitivity analysis of values at risk. Journal of Empirical Finance, 7(3-4):225–245.

Litterman, R. (1996). Hot spots™ and hedges. Journal of Portfolio Management, 23(5):52–75.

Martin, D. and Arora, R. (2017). Inefficiency of modified VaR and ES. Journal of Risk, 19(6):59–84.

Reid, S., Tibshirani, R., and Friedman, J. (2016). A study of error variance estimation in lasso regression. Statistica Sinica, 26:35–67.

Scaillet, O. (2004). Nonparametric estimation and sensitivity analysis of expected shortfall. Mathematical Finance, 14(1):115–129.

Schmidt, R., Hrycej, T., and Stützle, E. (2006). Multivariate distribution models with generalized hyperbolic margins. Computational Statistics & Data Analysis, 50(8):2065–2096.

Scott, R. C. and Horvath, P. A. (1980). On the direction of preference for moments of higher order than the variance. Journal of Finance, 35(4):915–919.

Stoyanov, S. V., Rachev, S. T., and Fabozzi, F. J. (2013a). CVaR sensitivity with respect to tail thickness. Journal of Banking & Finance, 37(3):977–988.

Stoyanov, S. V., Rachev, S. T., and Fabozzi, F. J. (2013b). Sensitivity of portfolio VaR and CVaR to portfolio return characteristics. Annals of Operations Research, 205(1):169–187.

Van der Weide, R. (2002). GO-GARCH: A multivariate generalized orthogonal GARCH model. Journal of Applied Econometrics, 17(5):549–564.

Zangari, P. (1996). A VaR methodology for portfolios that include options. RiskMetrics Monitor, First Quarter:4–12.

Zoia, M. G., Biffi, P., and Nicolussi, F. (2018). Value at risk and expected shortfall based on Gram-Charlier-like expansions. Journal of Banking & Finance, 93:92–104.

Zou, H. and Hastie, T. (2005). Regularization and variable selection via the elastic net. Journal of the Royal Statistical Society: Series B (Statistical Methodology), 67(2):301–320.

Zou, H., Hastie, T., and Tibshirani, R. (2007). On the "degrees of freedom" of the lasso. Annals of Statistics, 35(5):2173–2192.